Eur. Phys. J. C 49, 957–965 (2007)
DOI 10.1140/epjc/s10052-006-0179-1

THE EUROPEAN PHYSICAL JOURNAL C

Regular Article – Theoretical Physics

Factorization breaking in dijet photoproduction with a leading neutron

M. Klasen[1,2,a], G. Kramer[2]

[1] Laboratoire de Physique Subatomique et de Cosmologie, Université Joseph Fourier/CNRS-IN2P3, 53 avenue des Martyrs, 38026 Grenoble, France
[2] II. Institut für Theoretische Physik, Universität Hamburg, Luruper Chaussee 149, 22761 Hamburg, Germany

Received: 21 August 2006 / Revised version: 10 October 2006 /
Published online: 16 January 2007 –

Abstract. The production of dijets with a leading neutron in ep interactions at HERA is calculated in leading order and next-to-leading order of perturbative QCD using a pion-exchange model. Differential cross sections for deep-inelastic scattering and photoproduction are presented as a function of several kinematic variables. By comparing the theoretical predictions for DIS dijets to recent H1 data, the pion flux factor together with the parton distribution functions of the pion is determined. The dijet cross sections in photoproduction show factorization breaking if compared to the H1 photoproduction data. The suppression factor is $S = 0.48$ (0.64) for resolved (global) suppression.

PACS. 12.38.Bx; 13.60.-r

1 Introduction

In recent years, the validity of QCD factorization in hard diffractive scattering has become an important issue experimentally and theoretically. Factorization in hard diffraction means that the observed cross sections in hard diffractive processes can be calculated by a convolution of diffractive parton distributions with parton-level cross sections. Hard-scattering factorization has been proven by Collins [1–3] for inclusive diffractive deep-inelastic scattering (DIS), i.e. for the diffractive structure functions. It is supposed to be valid also for subprocesses like jet production and heavy-quark production in the DIS region. The proof of the factorization formula also appears to be valid for the direct photoproduction of jets and heavy quarks [1–3]. Factorization does not hold for hard processes in diffractive hadron–hadron scattering. Here, soft interactions between the two hadrons, and their remnants, occur in both the initial and final state, which prevents one from using the same steps as in the proof for diffractive DIS. Therefore, factorization fails also for resolved photoproduction. The failure of factorization in hadron–hadron scattering is observed experimentally [4]. The cross section for diffractive dijet production at CDF is suppressed relative to the prediction based on diffractive parton distribution functions (PDFs) from the H1 collaboration [5] by one order of magnitude [4]. The breaking of hard factorization in diffractive dijet photoproduction is also firmly established by analyses of H1 [6] and ZEUS [7] experimental data. Whether these experimental data are consistent with the breaking in the resolved component alone or whether this breaking occurs also in the direct photoproduction cross section is still not satisfactorily proven. It seems that the data are better described by a global suppression of the direct and resolved contribution by about a factor of two. It is important to note that this suppression is only visible if the data are compared to the next-to-leading order (NLO) QCD predictions as it was first shown by us in [8–10].

Factorization breaking is expected not only in the diffractive region, $x_{I\!P} \ll 1$, where $x_{I\!P}$ is the momentum fraction transferred to the exchanged particle in the t-channel, but also at larger values of $x_{I\!P}$, where Regge exchanges other than the pomeron occur between the initial- and final-state proton. These secondary Reggepole exchanges are not only present for $p \to p$ transitions but also in $p \to n$ transitions, in which pion exchange is strong. Therefore dijet photoproduction with a leading neutron could also be a candidate for factorization breaking as was already suggested in [8, 9]. Dijet photoproduction, $e^+ + p \to e^+ + n + \text{jet} + \text{jet} + X'$, with pion exchange has been studied in leading order (LO) and NLO in [11] and compared to ZEUS experimental data [12]. Recently the H1 collaboration has measured these dijet cross sections for photoproduction ($Q^2 < 0.01\,\text{GeV}^2$) and DIS ($Q^2 > 2\,\text{GeV}^2$) [13]. The photoproduction cross sections were compared to the NLO predictions of [11], and good agreement was found concerning the shape and normalization of distributions for various kinematic variables similar to the comparison done in [11] to the ZEUS

[a] e-mail: klasen@lpsc.in2p3.fr

data. Neither in [11] nor in [13] the factorization breaking of the dijet photoproduction cross sections has been investigated. This is difficult, since the breaking shows up dominantly in the normalization of the cross sections and to a much lesser extent in the shape of the distributions.

In the pion-exchange model, the normalization of the neutron-tagged cross sections depends first on the splitting function of a proton into a pion and a neutron $f_{\pi/p}(x_{\rm L},t)$. Here, $x_{\rm L}$ and t are the two variables which describe the proton–neutron vertex. $x_{\rm L}$ is the fraction of the initial-state proton energy transferred to the neutron, and t is the square of the momentum transfer between the proton and neutron. Second, the normalization depends on the parton distribution functions of the pion, for which several models exist in the literature [14–18].

The pion flux $f_{\pi/p}(x_{\rm L},t)$ can, in principle, be measured in charge-exchange processes in soft hadronic reactions, where an initial-state proton is transformed into a final-state neutron, $p\to n$, with small momentum transfer. A successful phenomenological description of the corresponding data has been given in the framework of reggeized isovector exchanges, such as π,ρ and a_2 with the pion dominating the $p\to n$ transition, in particular at small squared momentum transfer t between proton and neutron [19–23]. Unfortunately these cross sections are not given by pure Regge-exchange amplitudes. They are modified by soft rescattering of the incoming and outgoing hadrons, which influences the normalization of the cross sections, i.e. it leads to modified flux factors $f_{\pi/p}(x_{\rm L},t)$ due to the absorption of leading neutrons and the ingoing protons, which depends on $x_{\rm L}$ and t. Such corrections were studied some time ago by several authors [24, 25].

The pion PDFs are constrained by di-muon and prompt-photon production data from fixed target experiments that are sensitive to the valence-quark distribution in a Bjorken-x range relevant for dijet production on pions [14–18]. Unfortunately, these constraints are not very restrictive so that the existing parameterizations [14–18] differ in the relevant x-range, which leads to appreciable differences in the calculated dijet photoproduction cross sections [11].

The most direct way to determine the flux factor times the structure function of the pion $F_2^\pi(x,Q^2)$ is to measure the inclusive DIS cross section with a tagged neutron. On the basis of Collins' factorization proof, we expect in this case no absorptive interactions at high Q^2. Such cross sections for leading neutrons have been measured in ep-collisions at HERA [26–30]. Unfortunately these data have not been analyzed towards determining the PDFs of the pion, assuming a fixed ansatz for the $p\to n$ vertex, as it has been done towards the PDFs of the pomeron from diffractive semi-inclusive cross sections [5, 31]. Therefore we shall follow a different route. First, we assume one of the PDFs of the pion in the literature, for example those of Glück, Reya and Vogt (GRV) [16], and determine the normalization of $f_{\pi/p}(x_{\rm L},t)$ by comparing the NLO dijet cross sections for $Q^2>2\,{\rm GeV}^2$ to the data of the H1 collaboration [13]. With this $f_{\pi/p}(x_{\rm L},t)$ in conjunction with GRV's pion PDFs, we have calculated the NLO dijet cross section for photoproduction ($Q^2\simeq 0$) on the basis of [11] and compare them with the experimental results in [13]. Here the experimental tagged neutron DIS and photoproduction cross sections are obtained in a common analysis in the same region of the neutron kinematic variables. Second, we assume that the dijet production data in the DIS region are influenced very little by absorptive corrections, i.e. have no (or only a very small) breaking of factorization. Then the failure of our NLO photoproduction cross sections to describe the corresponding data of [13] will give us the amount of factorization breaking for photoproduction.

In Sect. 2, we shall describe the calculation of the dijet cross sections with a leading neutron, together with the kinematic variables, and define our input for the pion flux and the pion PDFs. The NLO cross sections are compared to several measured DIS cross sections from [13], so that our assumptions concerning $f_{\pi/p}(x_{\rm L},t)$ and the pion PDFs can be tested. Section 3 contains our results for the dijet cross sections in the $Q^2\simeq 0$ region and the comparison with the experimental data of [13]. On this basis we test also whether the factorization breaking can be attributed to the resolved component alone. In Sect. 4, we give a short summary and draw some conclusions.

2 Dijet cross sections in DIS

2.1 Kinematic variables and input

The event kinematics has already been described in [13]. Here we recall the definition of those variables which are needed in the calculations of the cross sections. The reaction

$$e^+(k)+p(P)\to e^+(k')+n(P')+X(p_{\rm X})\,, \qquad (1)$$

where X is the hadronic system containing at least two jets, is characterized by the four-momenta k and k' of the initial and scattered positron and by P and P', the four-momenta of the ingoing proton and outgoing neutron, respectively, as sketched in Fig. 1 (left). The positron–photon vertex is described by the exchanged photon virtuality Q^2 and the positron's inelasticity y,

$$Q^2=-q^2=-(k-k')^2\,,\quad y=\frac{Pq}{Pk}\,. \qquad (2)$$

In the H1 experiment [13], $2<Q^2<80\,{\rm GeV}^2$ and $0.1<y<0.7$ in the DIS region and $Q^2<10^{-2}\,{\rm GeV}^2$ and $0.3<y<0.65$ for the photoproduction selection. The protons at HERA have the energy $E_p=820\,{\rm GeV}$ and collide with $E_{\rm e}=27.6\,{\rm GeV}$ positrons.

The two variables, which describe the proton–neutron vertex, are the fraction $x_{\rm L}$ of the energy of the initial-state proton E_p carried by the neutron and the square of the momentum transfer t between the proton and the produced

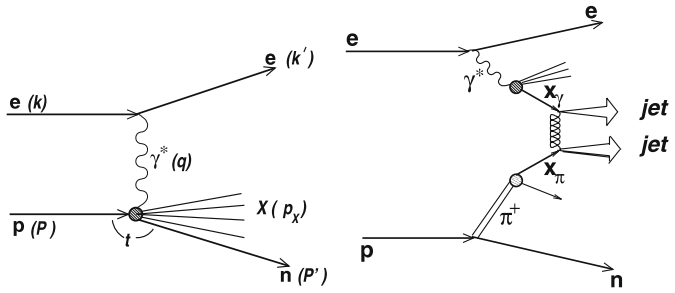

Fig. 1. Generic Feynman diagrams for the scattering process $e+p \to e+n+X$ (*left*) and for the production of two jets in the one-pion exchange model (*right*)

neutron,

$$x_{\mathrm{L}} = \frac{P'q}{Pq} \simeq \frac{E_n}{E_p}\,,$$
$$t = (P-P')^2 \simeq \frac{-p_{\mathrm{T}n}^2}{x_{\mathrm{L}}} - (1-x_{\mathrm{L}})\left(\frac{m_n^2}{x_{\mathrm{L}}} - m_p^2\right)\,, \quad (3)$$

where E_n is the neutron energy, $p_{\mathrm{T}n}$ is the momentum component of the neutron transverse to the direction of the ingoing proton, and m_n and m_p are the neutron and proton masses, respectively. x_{L} and t are determined from the measured energy and scattering angle of the leading neutron. In the H1 experiment $E_n > 500\,\mathrm{GeV}$ and $\theta_n < 0.8\,\mathrm{mrad}$.

In the pion-exchange model, the photon interacts with a pion emitted from the proton. In this model, the process $e^+ + p \to e^+ + n + \mathrm{jet} + \mathrm{jet} + X'$ as sketched in Fig. 1 (right) is described by the variable x_π, which, neglecting masses, is the fraction of the four-momentum of the pion $q' = P - P'$ participating in the hard interaction. It is related to x_p, the fraction of the four-momentum of the proton, which enters the hard interaction, by $x_p = x_\pi(1-x_{\mathrm{L}})$. x_{L} is related to $x_{I\!P}$ introduced in Sect. 1 in connection with diffractive jet production via $x_{\mathrm{L}} = 1 - x_{I\!P}$.

In the scattering of $2 \to 2$ massless partons, the fractions of the four-momenta $q = k - k'$ and $q' = P - P'$ transferred to the partons are given by

$$x_\gamma^{\mathrm{jet}} = \frac{\sum_{\mathrm{jets}} E_{\mathrm{T}}^{\mathrm{jet}} \mathrm{e}^{-\eta^{\mathrm{jet}}}}{2yE_e} \quad (4)$$

and

$$x_\pi^{\mathrm{jet}} = \frac{\sum_{\mathrm{jets}} E_{\mathrm{T}}^{\mathrm{jet}} \mathrm{e}^{\eta^{\mathrm{jet}}}}{2E_p(1-x_{\mathrm{L}})}\,, \quad (5)$$

so that

$$x_p^{\mathrm{jet}} = \frac{\sum_{\mathrm{jets}} E_{\mathrm{T}}^{\mathrm{jet}} \mathrm{e}^{\eta^{\mathrm{jet}}}}{2E_p}\,. \quad (6)$$

The sums in (4)–(6) run over the variables of the two jets in the final state. $E_{\mathrm{T}}^{\mathrm{jet}}$ and η^{jet} denote the transverse energies and pseudorapidities in the laboratory system. Strictly speaking, (4) is correct only for photoproduction, where $q^2 \simeq 0$, and furthermore $q'^2 = 0$. The energy fraction contributing by the exchanged virtual photon to the production of the dijets is x_γ^{jet}, whereas the corresponding contribution of the virtual pion (or possibly of a reggeized ρ or a_2) is x_π^{jet}. In (4), $E_\gamma = yE_{\mathrm{e}}$ is the energy of the ingoing virtual photon. In NLO, also three jets can be produced in the final state, but these contributions have been removed from the theoretical prediction in accordance with the experimental analysis, which contains only an exclusive dijet sample (see below).

As in the jet analysis of the experimental data [13], we use the cone algorithm with radius $R' = 1$ [32] for the jet definition and the combination of two partons into one jet in the NLO contributions of the DIS and the photoproduction sample. In our previous work [11], we had used the k_{T}-cluster algorithm instead. The jet finding is performed in the $\gamma^* p$ center-of-mass frame with transverse energies defined relative to the γ^* momentum axis. The laboratory pseudorapidity of each jet is restricted to the region $-1 < \eta^{\mathrm{jet}} < 2$. The transverse energies of the two jets with the largest E_{T} are constrained to the region $E_{\mathrm{T}}^{\mathrm{jet1}} > 7\,\mathrm{GeV}$ and $E_{\mathrm{T}}^{\mathrm{jet2}} > 6\,\mathrm{GeV}$ for both the DIS and the photoproduced jets in accordance with the requirement of asymmetric $E_{\mathrm{T}}^{\mathrm{jet}}$-cuts [33]. The calculated cross sections are restricted to the selection of exactly two jets, i.e. the rather small contribution of three jets with $E_{\mathrm{T}}^{\mathrm{jet3}} > 6\,\mathrm{GeV}$ is not included as in the experimental selection [13].

For the production of dijets in the DIS region, we consider only the contribution of the directly coupled γ^*, although at Q^2 as low as $2\,\mathrm{GeV}^2$ the resolved contribution starts to be relevant [34]. For the photoproduction of dijets we take into account the direct and the resolved process both in LO and NLO. The observable x_γ^{jet} is sensitive to the amount of direct and resolved processes.

In the pion-exchange model, the cross section for $\gamma^* p$ scattering to the final-state nX (see (1)) takes the form

$$\mathrm{d}\sigma(\gamma^* p \to nX) = f_{\pi/p}(x_{\mathrm{L}}, t)\mathrm{d}\sigma(\gamma^*\pi^+ \to X)\,, \quad (7)$$

where $f_{\pi/p}$ is the pion flux for the transition $p \to n + \pi^+$, and $\mathrm{d}\sigma(\gamma^*\pi^+ \to X)$ stands for the cross section of the hard γ^*-π^+ interaction. The splitting function or pion flux is usually parameterized by different forms. We choose

$$f_{\pi/p}(x_{\mathrm{L}}, t) = \frac{1}{4\pi}\frac{g_{n\pi p}^2}{4\pi}\frac{-t}{(m_\pi^2 - t)^2}(1-x_{\mathrm{L}})^{1-2\alpha_\pi(t)}[F(x_{\mathrm{L}}, t)]^2. \quad (8)$$

Here, $g_{n\pi p}$ is the coupling constant of the $n\pi p$ vertex, m_π is the pion mass and $\alpha_\pi(t) = \alpha'(t - m_\pi^2)$ is the Regge trajectory of the pion. $F(x_{\mathrm{L}}, t)$ is a form factor, which describes the off-shell behavior of the virtual pion and/or possible final-state rescattering effects of the neutron. We choose the so-called light-cone form factor

$$F(x_{\mathrm{L}}, t) = \exp[R^2(t - m_\pi^2)/(1-x_{\mathrm{L}})]\,. \quad (9)$$

This choice is usually associated with the flux without Regge trajectory factor, i.e. $\alpha' = 0$ in (8) [35], which would otherwise give a too steep p_{T}-dependence. The pion–nucleon

coupling constant is known from low-energy πN and NN scattering data. We take $g^2_{n\pi p}/4\pi = 2 \times 14.11$ [36]. Other choices of $F(x_L, t)$ have been used in the literature. We consider only the form in (9), since it has been used also in [13].

Another important input is the PDFs of the pion. For this several choices are available in the literature [14–18]. We choose the parameterization of Glück, Reya and Vogt (GRV) [16] which was also chosen in [13]. They provide PDFs in LO and NLO and also include the charm contribution. For the calculation of the photoproduction cross sections we need the PDFs of the photon for the resolved part. A popular parameterization is the one of Glück, Reya and Vogt (GRV) [37] which was also the choice in [13]. The $\Lambda_{\overline{\rm MS}}$ parameter, which we need in the LO and NLO formulas for α_s, is adjusted to the PDG 2006 edition [38] value for $\alpha_s(m_Z) = 0.1176$. This yields for four flavors $\Lambda^{(4)}_{\overline{\rm MS}} = 0.118\,\text{GeV}$ in LO and $\Lambda^{(4)}_{\overline{\rm MS}} = 0.307\,\text{GeV}$ in NLO. Of course, our NLO predictions for DIS and photoproduction dijet cross sections depend on this value. For the LO (NLO) predictions we use LO (NLO) hard scattering matrix elements with the one-loop (two-loop) formula for α_s and the $\Lambda^{(4)}_{\overline{\rm MS}}$ values given above. Unfortunately, the Λ values used for the evolution of the GRV pion and photon PDFs are somewhat different, namely 0.200 GeV in LO and NLO. In the case of photoproduction, the photon flux is calculated with the usual Weizsäcker–Williams approximation including the non-logarithmic corrections as calculated in [39]. The renormalization and factorization scales are equal to the maximum transverse energy of the outgoing jets. Now, all parameters and PDFs are specified except for the radius R in the light-cone form factor in (9). The value of this parameter will be fixed by comparison of the theoretical cross section in DIS dijet production with the data of [13], i.e. with the measured cross sections $\mathrm{d}\sigma/\mathrm{d}E_T^{\rm jet}$, $\mathrm{d}\sigma/\mathrm{d}\eta^{\rm jet}$, $\mathrm{d}\sigma/\mathrm{d}\log_{10}(x_\pi^{\rm jet})$, and $\mathrm{d}\sigma/\mathrm{d}Q^2$. In [13], the photoproduction dijet data have been described very well with the choice $R = 0.65\,\text{GeV}^{-1}$.

In addition to pion exchange, secondary Regge exchanges (as for example ρ and a_2) are possible. Such contributions could be disentangled by a careful study of the flux factor as a function of x_L and t (or p_{T_n}). Such data are not available. In [13], the neutron energy dependence of the DIS and photoproduction dijet events were measured. The uncorrected data were compared to a pion-exchange model within a Monte Carlo simulation that included detector effects. The photoproduction data are reasonably described in shape and magnitude, whereas the DIS data are reproduced quite well in shape, but somewhat overestimated in magnitude. We take these results for a good indication that pion exchange is dominating over ρ- and a_2-exchanges at least in the region of $x_L > 0.6$. Since additional ρ- and a_2-exchanges influence only the $p \to n$ flux factor, this factor should be the same for the DIS and photoproduced dijets in case of no factorization breaking.

2.2 DIS dijet cross sections

The calculations of the dijet cross sections in the DIS region have been performed with the NLO Monte Carlo program JETVIP [40]. This program calculates jet cross sections in LO and NLO in DIS using the so-called phase space slicing method with an invariant mass cut-off to cancel the infrared and collinear singularities. The program, originally constructed for jet production in $\gamma^* p$ interactions, could easily be modified for our purpose to calculate jet cross sections with a tagged neutron. The only change is that the PDFs of the proton are replaced by the PDFs of the pion times the pion flux.

Since the neutron kinematics is not fixed in detail by the experiment, we had to integrate over a finite region in x_L and t according to (3). We did this in accordance with the specifications of the H1 experimental analysis. Except for the outgoing positron and the leading neutron, the final state consists of two or three jets in addition to the remnant jet of the pion. The two-jet sample contains the bare parton jets from the LO and virtual NLO contributions and the two jets originating from the recombination of two partons in the three-parton contribution using the cone algorithm. Then we calculated the differential cross section $\mathrm{d}^2\sigma/\mathrm{d}E_T\mathrm{d}\eta$, where E_T and η are the transverse energy and the rapidity of the jets in the two- or three-jet sample with $E_T^{\rm jet1} > 7\,\text{GeV}$ and $E_T^{\rm jet2} > 6\,\text{GeV}$ and $E_T^{\rm jet3} < 6\,\text{GeV}$, i.e. from the three-jet sample the events with a hard jet with $E_T^{\rm jet3} > 6\,\text{GeV}$ are left out. This defines the exclusive dijet sample as in the analysis by H1 [13]. The cross section $\mathrm{d}\sigma/\mathrm{d}E_T\mathrm{d}\eta$ was integrated over the region $-1 < \eta^{\rm jet1,2} < 2$ to yield $\mathrm{d}\sigma/\mathrm{d}E_T$ and integrated over E_T with the asymmetric E_T-cut defined above to give us $\mathrm{d}\sigma/\mathrm{d}\eta^{\rm jet}$ and similarly for $\mathrm{d}\sigma/\mathrm{d}\log_{10}(x_\pi^{\rm jet})$ and $\mathrm{d}\sigma/\mathrm{d}Q^2$.

The results for $\mathrm{d}\sigma/\mathrm{d}E_T^{\rm jet}$, $\mathrm{d}\sigma/\mathrm{d}\eta^{\rm jet}$, $\mathrm{d}\sigma/\mathrm{d}\log_{10}(x_\pi^{\rm jet})$ and $\mathrm{d}\sigma/\mathrm{d}Q^2$ are shown in Fig. 2a–d. In these figures we have plotted the experimental data from [13] and three theoretical predictions, in LO and NLO with $R = 0.65\,\text{GeV}^{-1}$ and one in NLO with $R = 0.55\,\text{GeV}^{-1}$. For $R = 0.55\,\text{GeV}^{-1}$ we show also the scale variation in NLO by varying the scale in the interval $\mu/2$ to 2μ. It is seen quite clearly that the NLO prediction with $R = 0.65\,\text{GeV}^{-1}$ does not describe the data, whereas the prediction with $R = 0.55\,\text{GeV}^{-1}$ is in reasonable agreement with the measured cross sections. We can quantify these statements by calculating the $\chi^2_{\rm DF}$ for the two cases. For $R = 0.65\ (0.55)\,\text{GeV}^{-1}$ we get $\chi^2_{\rm DF} = 1.78\ (0.78)$ for 24 degrees of freedom. We observe that the NLO corrections are very important in all four distributions, as one can see by comparing the predictions for $R = 0.65\,\text{GeV}^{-1}$ in LO and NLO. Our theoretical predictions will be modified by hadronic corrections, which stand for the difference between jets from hadrons, on which the measured cross sections rely, and jets built out of partons which are the subject of the theoretical predictions. Unfortunately these hadronic corrections, which are usually obtained from Monte Carlo programs, which simulate LO cross sections with parton showering and parton-to-hadron transitions, are not available for the DIS dijet cross sections with tagged neutrons. From experience with such cross sections with tagged protons, we know that these corrections are of the order of 10%–20% except for the $x_\gamma^{\rm jet}$-distribution, which is very much changed by these corrections. Actually, $\mathrm{d}\sigma/\mathrm{d}x_\gamma$ has also been meas-

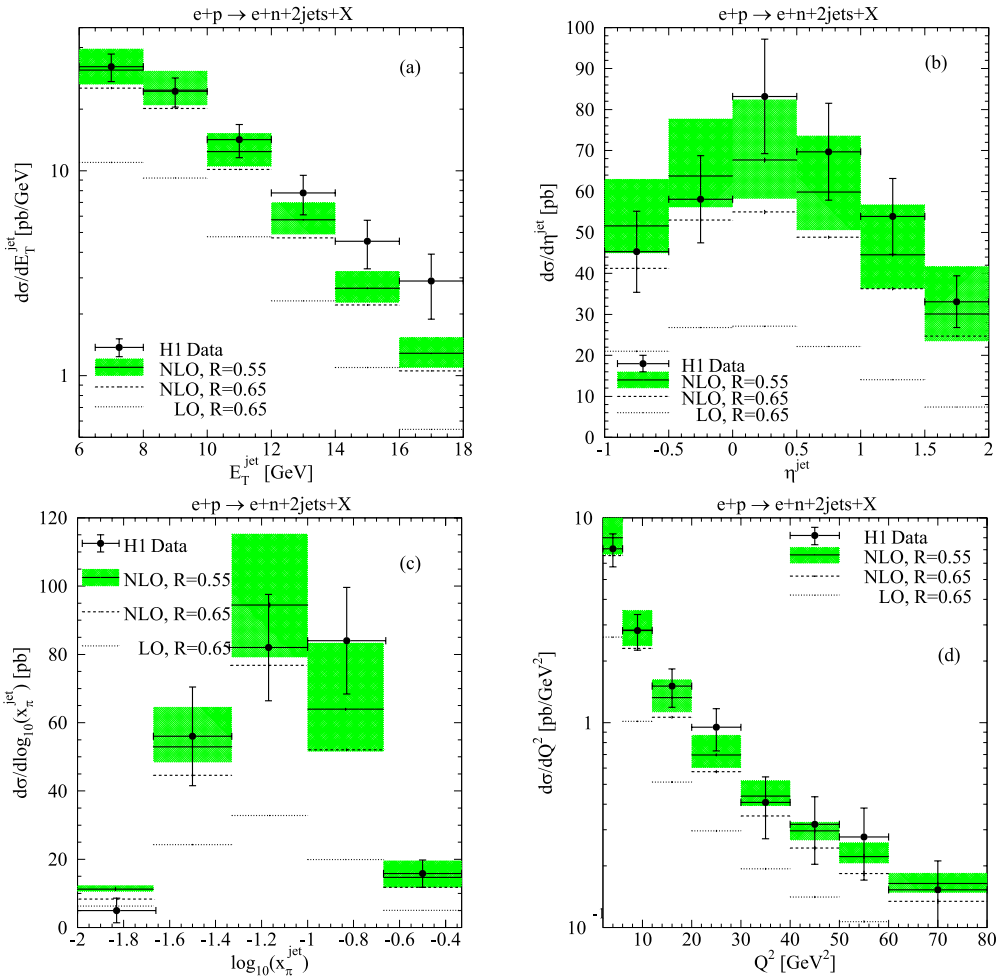

Fig. 2. Differential cross sections for deep-inelastic dijet production with a leading neutron. The H1 data are compared to perturbative QCD predictions in LO and NLO and with two different values for the pion–neutron radius R

ured in [13] for DIS dijets. Due to the sensitivity of this distribution to hadronic corrections, we did not consider this cross section suitable to give us a reliable R value.

3 Photoproduction cross sections

As in [11], the calculation of the photoproduction cross sections is based on the formalism fully described in our previous work [41, 42]. The cross sections which we shall evaluate are the same as in the DIS case described above. However, we now include also $\mathrm{d}\sigma/\mathrm{d}x_\gamma^{\mathrm{jet}}$ in order to see the contribution of the resolved part in the region $x_\gamma^{\mathrm{jet}} < 1$ more clearly. In the following we show the results for $\mathrm{d}\sigma/\mathrm{d}E_{\mathrm{T}}^{\mathrm{jet}}$, $\mathrm{d}\sigma/\mathrm{d}\eta^{\mathrm{jet}}$, $\mathrm{d}\sigma/\mathrm{d}x_\gamma^{\mathrm{jet}}$ and $\mathrm{d}\sigma/\mathrm{d}\log_{10}(x_\pi^{\mathrm{jet}})$ in Fig. 3a–d. In these figures, four different predictions are plotted and compared with the data from [13]. Three predictions are in NLO, one with the radius $R = 0.55\,\mathrm{GeV}^{-1}$, where hadronic corrections [13, 43] are included, and two with $R = 0.65\,\mathrm{GeV}^{-1}$ with and without hadronic corrections, and one is in LO with $R = 0.65\,\mathrm{GeV}^{-1}$ without hadronic corrections. The LO prediction is far off the experimental data showing that only NLO predictions are relevant and that the K-factor (K = NLO/LO) is large. For the $E_{\mathrm{T}}^{\mathrm{jet}}$-distribution in Fig. 3a, the prediction with $R = 0.55\,\mathrm{GeV}^{-1}$, where the shaded band gives the scale dependence of the cross sections, lies always above the data points except for the two largest E_{T}-bins. The prediction with $R = 0.65\,\mathrm{GeV}^{-1}$ agrees much better with the data in agreement with the results of [13]. In [13] the cross sections are somewhat smaller, since there α_{s} is smaller due to the choice of a smaller $\Lambda^{(4)}_{\overline{\mathrm{MS}}}$ value (0.200 GeV). From this figure, it is clear already that the radius $R = 0.55\,\mathrm{GeV}^{-1}$ gives a bad description of the H1 data and a reasonable agreement would be possible only for $R \geq 0.65\,\mathrm{GeV}^{-1}$. This is seen even more clearly in Fig. 3b–d, where the η^{jet}, x_γ^{jet} and $\log_{10}(x_\pi^{\mathrm{jet}})$ distributions are compared to the measured cross sections in [13]. The predictions lie above the data points, even if the theoretical error estimated by the scale dependence is taken into account. To reproduce the data in Fig. 3a–d a radius larger than $R = 0.65\,\mathrm{GeV}^{-1}$ would be needed. However, the radius $R = 0.55\,\mathrm{GeV}^{-1}$ was fixed by the DIS dijet cross sections. Our results in Fig. 3a–d, when compared to the photoproduction data of the H1 collaboration, demonstrate that they cannot be explained with the same pion flux plus pion PDFs. i.e. with $R = 0.55\,\mathrm{GeV}^{-1}$. This shows us that factorization breaking is present in photoproduction of dijets with a leading neutron with a breaking factor of $S \simeq 0.6$.

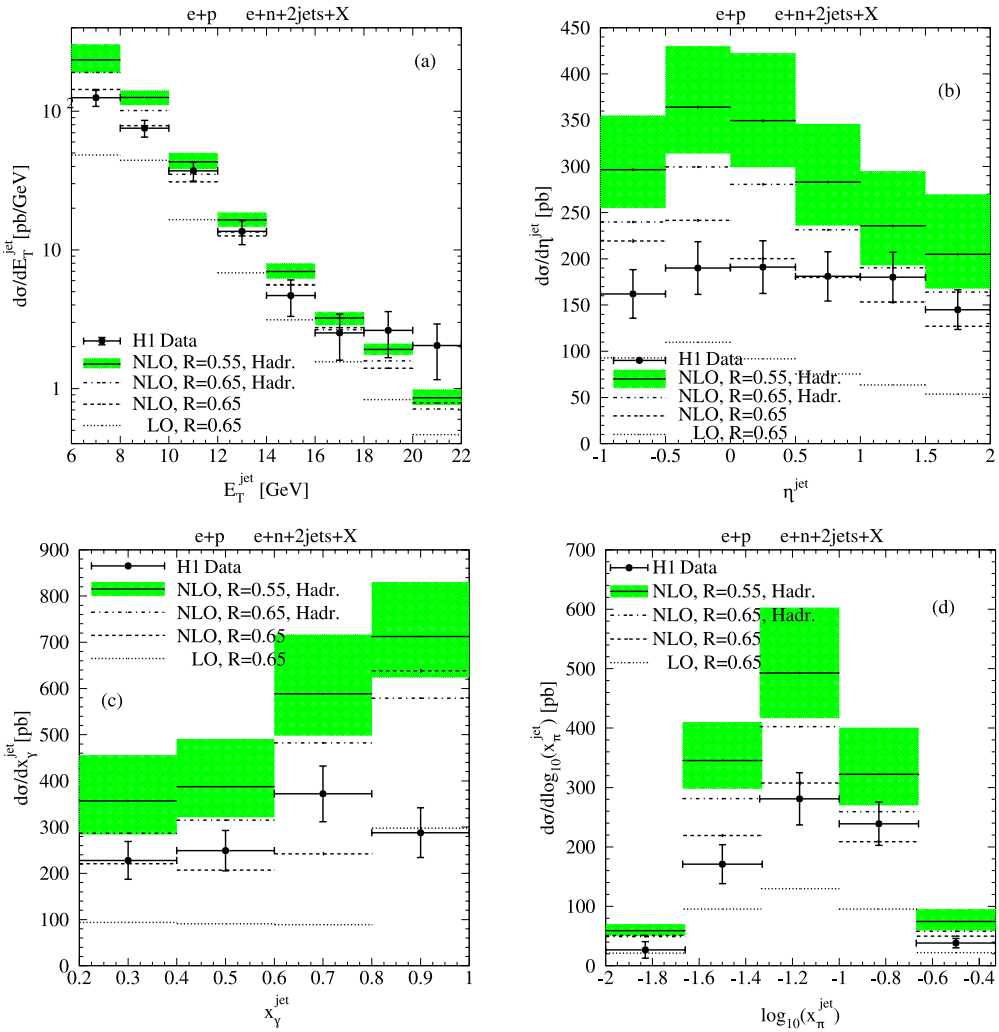

Fig. 3. Differential cross sections for dijet photoproduction with a leading neutron. The H1 data are compared to perturbative QCD predictions in LO and NLO and with two different values for the pion–neutron radius R

This breaking factor changes somewhat from cross section to cross section and as a function of the kinematic variables.

The details are shown in Fig. 4a–d, where we show the ratio H1 data/theory for the four cross sections with $R = 0.55\,\mathrm{GeV}^{-1}$, with and without hadronic corrections. In addition to the ratios following from the results in Fig. 3a–d, we show in Fig. 4a–d also another ratio, where the theoretical prediction is again obtained with $R = 0.55\,\mathrm{GeV}^{-1}$ including hadronic corrections, but now with a suppression factor $S = 0.48$ applied to the resolved cross section together with the μ_γ scale-dependent part of the NLO corrections to the direct cross section. Here, μ_γ is the factorization scale of the photon vertex. This additional suppression in the direct cross section introduced in [44] serves the purpose to eliminate the μ_γ-dependence of the sum of the direct and resolved cross section. We see from Fig. 4a–d that this ratio lies near to one if we take into account the scale variation of the theoretical prediction. The x_γ^{jet}-distribution yields values for this ratio larger than one (except for the last bin), which overlap, however, with the scale variation band. It is known that the x_γ^{jet}-distribution suffers from rather large hadronic corrections as seen for example in Fig. 3c, where the correction in the bin $x_\gamma^{\mathrm{jet}} \in [0.6; 0.8]$ is as large as a factor of two.

The two suppression factors, $S \simeq 0.6$ for the full direct and resolved contributions or $S = 0.48$ for the resolved and initial-state singular part of the direct contribution, can be compared with the suppression factor obtained in [45, 46]. In this work, the spectra of leading neutrons, both in photoproduction and in DIS, were studied and compared to recent ZEUS experimental data [26, 28–30]. It was found that the photoproduction cross section on the basis of the pion-exchange model agreed with the data if it was reduced by a factor of about 0.4. This factor could be quite well explained by absorptive corrections to pion exchange and can be compared with the suppression factor of 0.48 for the resolved/direct-IS components. Furthermore, it must be emphasized that the absorptive corrections for the total photoproduction cross section with a tagged neutron may differ from the absorptive corrections for the production of a pair of high-E_{T} jets, even in the resolved case.

In Fig. 5, we show separately the $E_{\mathrm{T}}^{\mathrm{jet}}$-distribution as measured by the H1 collaboration and compare it to theoretical NLO QCD predictions including hadronization

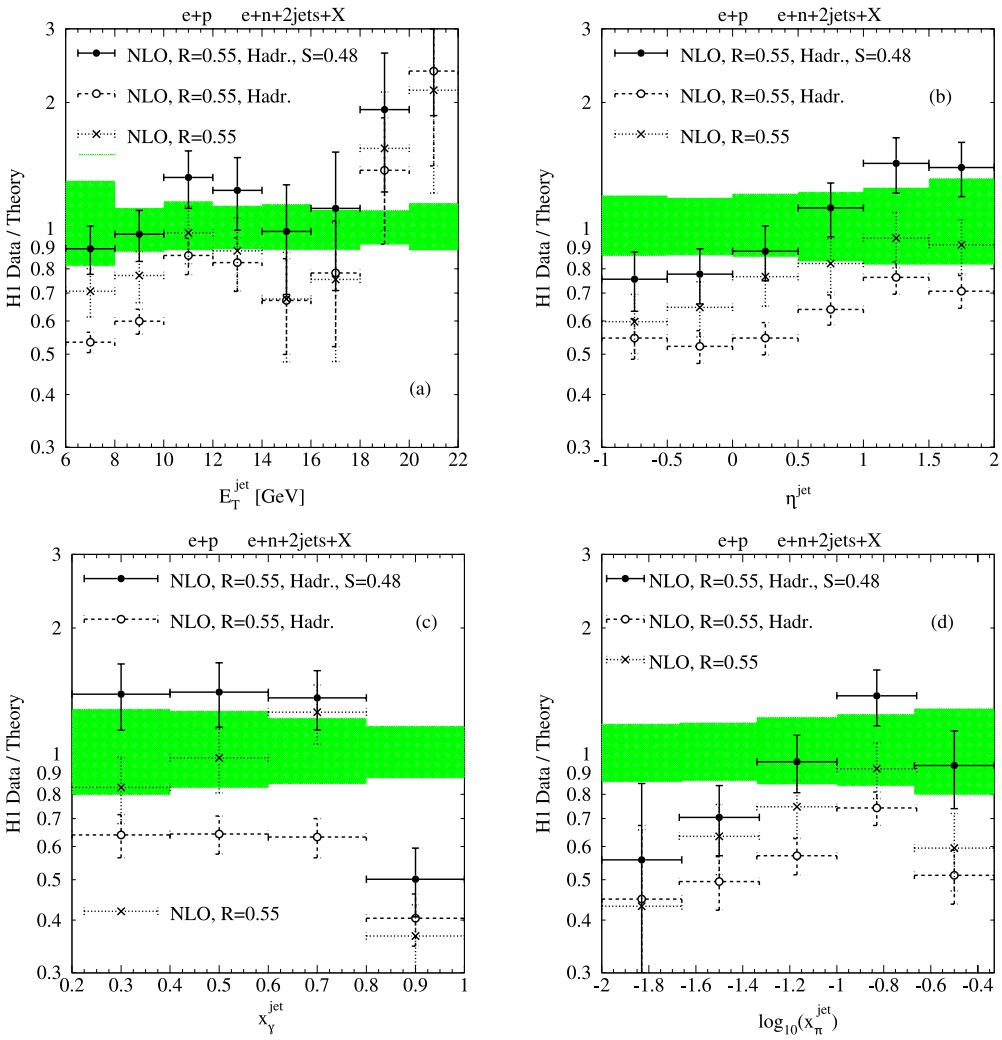

Fig. 4. Ratios of H1 data over NLO QCD for dijet photoproduction with a leading neutron, with and without hadronization corrections and including (*full points/lines*) a suppression factor S for the resolved component and its scale-dependent direct NLO counterpart

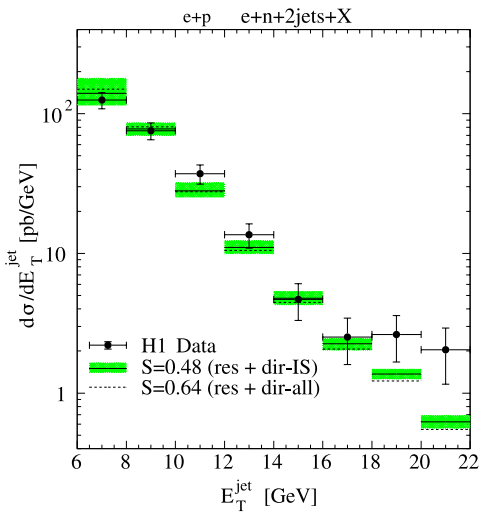

Fig. 5. E_T^{jet}-distribution of photoproduced dijets with a leading neutron. The H1 data are compared to NLO QCD calculations corrected for hadronization effects in the pion-exchange model with pion–neutron radius $R = 0.55\,\mathrm{GeV}^{-1}$ and suppression of the resolved/direct initial-state contributions (*full*) and of all direct and resolved photon contributions (*dashed*)

corrections and using the radius $R = 0.55\,\mathrm{GeV}^{-1}$. In the full histogram, we test the hypothesis of suppressing only the resolved (and direct initial-state) contributions with a factor $S = 0.48$ and obtain quite a reasonable value of $\chi^2_{\mathrm{DF}} = 1.2$. The shaded band indicates again the theoretical uncertainty coming from simultaneous variation of the renormalization and factorization scales by a factor of two around the central scale. It overlaps with the experimental error bars in all but the highest two bins, whose precision is obviously limited by statistics. In contrast, the dashed histogram tests the hypothesis of suppressing all direct and resolved contributions with a fitted factor $S = 0.64$, as proposed in the H1 analysis of diffractive dijet photoproduction, leading to a higher value of $\chi^2_{\mathrm{DF}} = 1.7$. We take this as an indication that the first hypothesis describes this most robust (and exponentially falling) distribution better.

Finally, we wish to comment on our earlier analysis [11] of the photoproduction dijet cross sections as measured by the ZEUS collaboration several years ago [12]. At this time, data on dijets with tagged neutrons in DIS were not available. Therefore, we fitted the pion–neutron radius R of the light-cone form factor to the ZEUS data

with the result $R = 0.5\,\mathrm{GeV}^{-1}$. As shown in this work, the H1 photoproduction data [13] are badly described with this radius. The reason for this mismatch is the fact that in [11] we have chosen different parameterizations of the pion PDFs, i.e. SMRS [17] versus GRV [16], and of the photon PDFs, i.e. GS96 [47] versus GRV [37]. In particular, the choice of the pion PDFs has a strong influence on the absolute value of the cross section (see for example Fig. 3 in [11]). The ZEUS collaboration demonstrated in 2002 [28] that the shape of their measured F_2^π-distribution agrees quite well with the GRV parameterization and much less with SMRS. Furthermore, the normalization of the theoretical dijet cross section was influenced by the choice of the difference in the E_T-cuts for the two jets, which was set to zero in the analysis of the experimental data.

4 Conclusion

In summary, we have performed a comprehensive NLO QCD analysis of dijet production with a leading neutron in both DIS and photoproduction. We emphasized the question whether factorization breaking occurs not only in diffractive photoproduction, but also in photoproduction with $p \to n$ transitions. Assuming that the latter are dominated by one-pion exchange and well described by GRV pion PDFs and a light-cone flux factor, we were able to fit its free parameter, the pion–neutron radius R, to recent H1 DIS data with the result $R = 0.55\,\mathrm{GeV}^{-1}$ for $\chi^2_\mathrm{DF} = 0.78$ and 24 degrees of freedom. In contrast, a radius of $R = 0.65\,\mathrm{GeV}^{-1}$ as used by the H1 collaboration leads to a considerably larger χ^2_DF of 1.78.

When applying the fitted radius of $R = 0.55\,\mathrm{GeV}^{-1}$ to our NLO QCD predictions for dijet photoproduction with a leading neutron, we seriously overestimate the corresponding H1 data. We therefore conclude that factorization breaking occurs not only in diffractive $ep \to e'pX$, but also in $ep \to e'nX$ scattering. Only after including absorptive corrections, a good phenomenological description of the H1 data can be obtained. A suppression of resolved photoproduction and its factorization-scale-dependent direct NLO counterpart only with a suppression factor of $S = 0.48$ seems to be favored over a global suppression of all direct and resolved contributions with a suppression factor of $S = 0.64$, at least in the steeply falling $E_\mathrm{T}^\mathrm{jet}$-distribution, where we obtain values of $\chi^2_\mathrm{DF} = 1.2$ versus 1.7.

Acknowledgements. M.K. gratefully acknowledges the hospitality of the Institute of Theoretical Physics at the University of Göttingen, where part of this work has been completed.

References

1. J. Collins, Phys. Rev. D **57**, 3051 (1998)
2. J. Collins, Phys. Rev. D **61**, 019 902(E) (2000)
3. J. Collins, J. Phys. G **28**, 1069 (2002)
4. CDF Collaboration, T. Affolder et al., Phys. Rev. Lett. **84**, 5043 (2000)
5. H1 Collaboration, Abstract 980, contributed to the 31st International Conference on High Energy Physics (ICHEP 2002), Amsterdam, July 2002
6. H1 Collaboration, Abstract 6-0177, contributed to the 32nd International Conference on High Energy Physics (ICHEP 2004), Beijing, August 2004
7. ZEUS Collaboration, Abstract 6-0249, contributed to the 32nd International Conference on High Energy Physics (ICHEP 2004), Beijing, August 2004
8. M. Klasen, G. Kramer, hep-ph/0401202
9. M. Klasen, G. Kramer, Proceedings of the 12th International Workshop on Deep Inelastic Scattering (DIS 2004), ed. by D. Bruncko, J. Ferencei, P. Strizzenec, Kosice, Inst. Exp. Phys. SAS, 2004, p. 492
10. M. Klasen, G. Kramer, Eur. Phys. J. C **38**, 93 (2004)
11. M. Klasen, G. Kramer, Phys. Lett. B **508**, 259 (2001)
12. ZEUS Collaboration, J. Breitweg et al., Nucl. Phys. B **596**, 3 (2001)
13. H1 Collaboration, A. Aktas et al., Eur. Phys. J. C **41**, 273 (2005)
14. J.F. Owens, Phys. Rev. D **30**, 943 (1984)
15. P. Aurenche, R. Baier, M. Fontannaz, M.-N. Kienzle-Focacci, M. Werlen, Phys. Lett. B **233**, 519 (1989)
16. M. Glück, E. Reya, A. Vogt, Z. Phys. C **53**, 651 (1992)
17. P.J. Sutton, A.D. Martin, R.G. Roberts, W.J. Stirling, Phys. Rev. D **45**, 2349 (1992)
18. M. Glück, E. Reya, I. Schienbein, Eur. Phys. J. C **10**, 313 (1999)
19. J. Engler et al., Nucl. Phys. B **84**, 70 (1975)
20. W. Flauger, F. Mönnig, Nucl. Phys. B **109**, 347 (1976)
21. S.J. Barish et al., Phys. Rev. D **12**, 1260 (1975)
22. B. Robinson et al., Phys. Rev. Lett. **34**, 1475 (1975)
23. Y. Eisenberg et al., Nucl. Phys. B **135**, 189 (1978)
24. N.N. Nikolaev, J. Speth, B.G. Zakharov, hep-ph/9708290
25. U.D. Alesio, H.J. Pirner, Eur. Phys. J. A **7**, 109 (2000)
26. ZEUS Collaboration, M. Derrick et al., Phys. Lett. B **384**, 388 (1996)
27. H1 Collaboration, C. Adloff et al., Eur. Phys. J. C **6**, 587 (1999)
28. ZEUS Collaboration, S. Chekanov et al., Nucl. Phys. B **637**, 3 (2002)
29. ZEUS Collaboration, S. Chekanov et al., Phys. Lett. B **610**, 199 (2005)
30. M. Soares for the ZEUS Collaboration, Contribution to the 14th International Workshop on Deep Inelastic Scattering (DIS 2006), Tsukuba, Japan, April 2006
31. H1 Collaboration, A. Aktas et al., Eur. Phys. J. C **48**, 715 (2006)
32. J.E. Huth et al., Towards a standardization of jet definitions, Fermilab-Conf. 90/249E (1990)
33. M. Klasen, G. Kramer, Phys. Lett. B **366**, 385 (1996)
34. M. Klasen, G. Kramer, Phys. Rev. Lett. **93**, 232 002 (2004)
35. H. Holtmann et al., Phys. Lett. B **338**, 363 (1994)
36. T.E. Ericson, B. Loiseau, A.W. Thomas, Phys. Rev. C **66**, 014 005 (2002)
37. M. Glück, E. Reya, A. Vogt, Phys. Rev. D **46**, 1973 (1992)
38. W.M. Yao et al., J. Phys. G **33**, 1 (2006)
39. S. Frixione, M.L. Mangano, P. Nason, G. Ridolfi, Phys. Lett. B **319**, 339 (1993)
40. B. Pötter, Comput. Phys. Commun. **133**, 105 (2000)

41. M. Klasen, G. Kramer, Z. Phys. C **76**, 67 (1997)
42. M. Klasen, T. Kleinwort, G. Kramer, Eur. Phys. J. C **1**, 1 (1998)
43. A. Bunyatian, private communication
44. M. Klasen, G. Kramer, J. Phys. G **31**, 1 (2005)
45. A.B. Kaidalov, V.A. Khoze, A.D. Martin, M.G. Ryskin, Eur. Phys. J. C **47**, 385 (2006)
46. V.A. Khoze, A.D. Martin, M.G. Ryskin, Eur. Phys. J. C **48**, 797 (2006)
47. L.E. Gordon, J.K. Storrow, Nucl. Phys. B **489**, 405 (1997)